Evolution with Composition of the d-Band Density of States at the Fermi Level in Highly Spin Polarized $Co_{1-x}Fe_xS_2$

P. L. Kuhns,[1] M. J. R. Hoch,[1] A. P. Reyes,[1] W. G. Moulton,[1] L. Wang,[2] and C. Leighton[2]
[1]National High Magnetic Field Laboratory, Florida State University, Tallahassee, Florida 32310, USA
[2]Department of Chemical Engineering and Materials Science, University of Minnesota, Minneapolis, Minnesota 55455, USA
(Received 8 August 2005; revised manuscript received 30 January 2006; published 28 April 2006)

Highly spin polarized (SP) and half-metallic ferromagnetic systems are of considerable current interest and of potential importance for spintronic applications. Recent work has demonstrated that $Co_{1-x}Fe_xS_2$ is a highly polarized ferromagnet (FM) where the spin polarization can be tuned by alloy composition. Using ^{59}Co FM-NMR as a probe, we have measured the low-temperature spin relaxation in this system in magnetic fields from 0 to 1.0 T for $0 \leq x \leq 0.3$. The ^{59}Co spin-lattice relaxation rates follow a linear T dependence. Analysis of the data, using expressions for a FM system, permits information to be obtained on the d-band density of states at the Fermi level. The results are compared with independent density of states values inferred from electronic specific heat measurements and band structure calculations. It is shown that FM-NMR can be an important method for investigating highly SP systems.

DOI: 10.1103/PhysRevLett.96.167208 PACS numbers: 85.75.Dd, 71.20.Be, 76.60.Es

Highly spin polarized (SP) ferromagnets (FMs) are a special class of ferromagnetic materials where the density of states (DOS) $\rho(E_F)$ at the Fermi level E_F is finite for one spin orientation and close to zero for the other, producing conduction band electron spin polarization (P) near 100% [1–3]. These highly SP FMs offer exciting opportunities for device development [4,5] and may be regarded as a new state of matter with interesting properties [6]. Many predictions of highly SP systems that are close to half-metallic FMs have been made but very few have been verified experimentally. Systems that have been found experimentally to have very high SP at low temperatures include the metal oxides Fe_3O_4 [7] and CrO_2 [8–10] and the doped manganites $La_{1-x}Sr_xMnO_3$ [11,12]. Recent theoretical and experimental work [13–15] has shown that the itinerant FM compounds $Co_{1-x}Fe_xS_2$ ($0.07 < x < 0.5$) are highly SP. Pure FM CoS_2, with the electronic configuration $t_{2g}{}^6 e_g{}^1$, is theoretically predicted to be highly SP [16,17] but low-temperature experiments [18] involving point contact Andréev reflection (PCAR) show a SP of 56%. Local spin density approximation (LSDA) [13–15] calculations suggest that, in the alloyed material $Co_{1-x}Fe_xS_2$, the DOS evolves with x such that E_F decreases towards the low energy edge of the minority (down) spin sub-band, while there is a large DOS at E_F for the majority (up) spins. The SP can therefore be tuned by alloy composition and P values of 100% are predicted for $x \geq 0.25$. PCAR measurements made at 4.2 K [15] show that P increases with x, reaching a maximum value of 85% for $x = 0.15$ before decreasing slightly at higher x. The tunability of P by solid state alloying of CoS_2 with FeS_2 offers important opportunities in basic and applied research. We note that highly SP systems have been found to lose their large polarizations at temperatures far below T_C. This is attributed to collective low-energy excitations [19,20].

We use ^{59}Co NMR to examine the low-temperature properties of $Co_{1-x}Fe_xS_2$ polycrystals with composition and show that nuclear spin-lattice relaxation in FM d-band metals provides a novel means for studying the DOS $\rho(E_F)$ in this system. In conjunction with other measurements of the spin polarization, important information on the evolution of the band structure with x is obtained. In contrast to transport measurements, NMR spin-lattice relaxation times provide access to the thermodynamic DOS that can be directly compared with electronic specific heat capacity determinations and with band structure calculations.

Preparation of polycrystalline $Co_{1-x}Fe_xS_2$ samples was carried out by means of a three-stage synthesis procedure described previously [15,18]. Care was taken to ensure stoichiometry of the polycrystalline material and to avoid sulfur deficiency. Characterization by means of x-ray diffraction, scanning electron microscopy, and energy dispersive analysis of x rays have shown that they are single phase with a grain size of order 10 μm [15]. In order to study details of the hyperfine interaction in the parent material, a stoichiometric single crystal of CoS_2 was grown by the chemical vapor transport method. Details will be published elsewhere.

^{59}Co NMR line shape and relaxation measurements were made using a computer controlled pulsed spectrometer and an untuned low-temperature probe. The spectral line shapes were determined by integrating signal-averaged spin echoes and scanning the frequency over the spectral range. Probe response was experimentally calibrated over the frequency range of the ^{59}Co signals in CoS_2 and $Co_{1-x}Fe_xS_2$ (40–90 MHz) and showed that no corrections to spectra were necessary. Spin-lattice relaxation times (T_1) were obtained using the standard saturation comb, spin echo signal recovery technique [21]. Single exponentials gave good fits to the nuclear magnetization recovery curves. Spin-spin relaxation time (T_2) values were measured using integrated spin echoes that followed single exponential decay with pulse spacing. Experiments were carried out with the sample either in zero magnetic

field or in a small applied field in the range 0.1–1 T. Application of fields $H > 0.15$ T is sufficient to saturate the magnetization in these soft magnetic materials and to eliminate domain wall effects [22]. Specific heat measurements were made using standard relaxation techniques in a Quantum Design PPMS. The electronic contribution was extracted from the low-temperature data.

The electron density distribution in CoS_2, determined by high-resolution single crystal x-ray diffraction [23], suggests that the symmetry of the electron distribution around the metal ions is very close to cubic. Polarized neutron diffraction measurements on single crystal samples of CoS_2 [24,25] show that, while this material is an itinerant FM, the delocalized magnetic moment in the regions between the Co ions is very small compared to that in the FM transition metals. The moment is largely localized around the Co nuclei and is aspherical, with ~69% of the $3d$ electrons occupying e_g orbitals. Inelastic neutron scattering experiments have confirmed that CoS_2 is an itinerant FM [26].

A previous zero field NMR investigation on a powder sample of CoS_2 attributed the two spectral peaks to anisotropic hyperfine interactions [27,28]. In an effort to understand the spectra in greater detail, we have made NMR measurements on the single crystal CoS_2 sample at two orientations with respect to the applied magnetic field. Frequency swept line shape measurements, made as a function of field H ($0 \leq H \leq 1$ T) along the [001] and [111] directions, show that, in contrast to the previous interpretation [27,28], the spectral shape is due to four nonequivalent hyperfine principal axes directed along [111] at Co sites, as determined by site symmetry. We have used a hyperfine model based on this finding to fit the center frequencies of the Gaussian spectral peaks as a function of the direction of the local effective magnetic field. Axial symmetry is assumed for the hyperfine coupling. Four peak center frequencies are obtained with H along [001] and [111] directions. By combining the hyperfine field at each Co site with the applied field, and allowing for the change in domain structure as H is increased from 0 to 0.15 T, the NMR frequency corresponding to each site may be calculated as a function of H. The fits obtained are shown in Fig. 1(b) for the [001] orientation and are in good agreement with the experimental values. For $H > 0.15$ T, the frequency f for each component is given by $f = f_0 - {}^{59}\gamma H$, where f_0 is the intercept, showing that the hyperfine field aligns antiparallel to H.

The ^{59}Co spectra for polycrystalline $Co_{1-x}Fe_xS_2$ for $x =$ 0 to 0.3 are shown in Fig. 1(a) for $H = 0.2$ T at 4.2 K. The $x = 0$ spectrum consists of a broad main peak and a secondary shoulder peak. The complications of signal from domain walls are removed above 0.15 T. The spectra for the Fe substituted material progressively broaden with increasing x and this is attributed to an increased distribution of hyperfine fields and/or anisotropy produced by alloying. Gaussian fits to the main peak and the shoulder feature give a good representation of the spectra for the

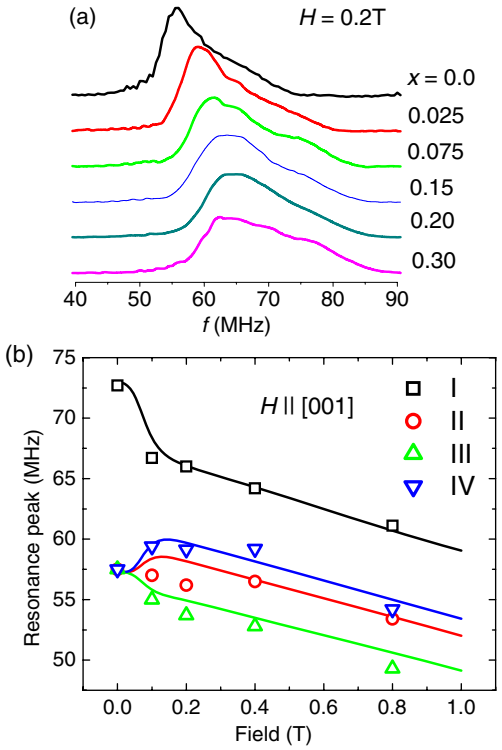

FIG. 1 (color online). (a) Waterfall plot (each 40–90 MHz) of ^{59}Co NMR spectra ($0.0 \leq x \leq 0.3$) in sintered $Co_{1-x}Fe_xCoS_2$ samples at 4.2 K. The spectra broaden and shift with increasing x. (b) The fitted resonance peak frequencies for the CoS_2 ($x = 0$) single crystal plotted as a function of external field along the [001] direction. The four peaks correspond to four crystallographically distinct Co atoms whose local symmetries lie along the [111] directions (labeled by Roman numerals). Domain walls are swept out above 0.15 T. Lines are fit to an anisotropic hyperfine field model.

alloyed material. The spectral centroid frequency f_c, obtained from the first moment of the line, increases with x in the range $0 < x < 0.1$ before reaching an approximately constant value. This behavior correlates with the dependence on x of the low-temperature reduced magnetization M (of the Co ions) consistent with the $H_{hf} \propto |M|$ at the ^{59}Co sites.

Spin-lattice relaxation rates $1/T_1$ are plotted in Fig. 2 as a function of T for samples with various x values and in all cases have the form $1/T_1 = \kappa T$, for the range shown, with κ a constant for each value of x [29]. Experimental values for κ are shown versus x in the inset in Fig. 2. Following an initial decrease κ reaches a plateau value. At much higher temperatures, $T > T_C/2$, the relaxation rate increases more rapidly than predicted by the linear T relation. Other relaxation mechanisms, involving spin wave excitations, for example, become important in this range. The spin-spin relaxation rate $1/T_2$ shows quite different behavior than that found for $1/T_1$ and is approximately x and T independent below 10 K, with an increase in the rate at higher temperatures. This behavior suggests that at these temperatures the Suhl-Nakamura virtual magnon mechanism [30]

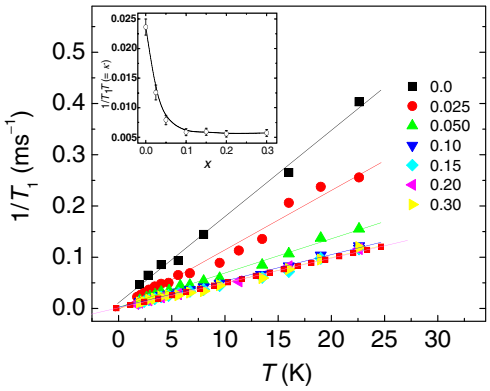

FIG. 2 (color online). ^{59}Co spin-lattice relaxation rate $1/T_1$ vs T for single crystal CoS_2 and sintered $Co_{1-x}Fe_xCoS_2$ samples with various x values. The inset shows the product $\kappa = 1/T_1T$ as a function of x.

plays a dominant role in spin-spin relaxation, as found, for example, in Co metal [31] and provides additional evidence for spin wave excitations in this highly SP system.

The T_1 data were analyzed using expressions based on the theory developed by Obata [32] for d-band metals and Moriya [33] for d-band FM. The relaxation mechanism involves fluctuating orbital currents and dipolar interactions due to electrons at the Fermi level. We consider the contributions to ^{59}Co spin-lattice relaxation in d-band FM:

$$\frac{1}{T_1} = \frac{1}{T_1^{\mathrm{orb}}} + \frac{1}{T_1^{\mathrm{dip}}} + \frac{1}{T_1^{\mathrm{cp}}}, \qquad (1)$$

with the superscripts designating orbital (orb), dipolar (dip) and core polarization (cp) mechanisms. Contact hyperfine interactions due to s electrons are not considered because ionization to form Co^{2+} removes s states. It is difficult to determine the core polarization contribution $1/T_1^{\mathrm{cp}}$ reliably but previous work on a variety of systems suggests that this contribution is negligibly small compared to the orbital or dipolar contributions [33,34]. We assume that, for the present highly SP systems, we can neglect this mechanism. Quadrupolar relaxation contributions are negligible, particularly at the low temperatures used in this work [33].

Using the Obata-Moriya approach, the orbital and dipolar contributions in this highly correlated electron system may be written in the tight binding approximation, as [32–34]

$$\frac{1}{T_1T} = 4\pi\gamma_S^2\gamma_I^2\hbar^3 k_{\mathrm{B}}\langle 1/r^3\rangle_F^2[\rho_\uparrow^2(E_F) + \rho_\downarrow^2(E_F)]F(\Gamma), \quad (2)$$

with γ_S the electron gyromagnetic ratio, $\langle 1/r^3\rangle_F$ the inverse cube of the d-electron radii averaged over the Fermi surface (assumed the same for up or down spins), $F(\Gamma)$ a function discussed below, and $\rho_{\uparrow(\downarrow)}(E_F)$ the density of d-band states for up (down) spins at the Fermi level, with normalization for a given spin orientation specified by $\int \rho_\uparrow(\varepsilon)d\varepsilon = 1$ [32]. Separation of the spin band contributions follows from the significant differences of the Fermi surfaces for up and down spins. In the case of a SP system, the Fermi surface for one of the spin bands shrinks and the corresponding density of states becomes less important in Eq. (2). In particular, for highly SP systems one spin subband will be dominant. The function $F(\Gamma)$ depends on the atomic d-electron wave functions belonging to the irreducible representations Γ of the cubic point group that are used in constructing the Bloch functions. As shown by Obata [32] and Moriya [33], $F(\Gamma) \sim 0$ for orbital relaxation when there is only a small admixture of $\Gamma_5(t_{2g})$ and the Bloch functions involve primarily the two $\Gamma_3(e_g)$ atomic functions. This limit applies to CoS_2 ($t_{2g}{}^6e_g{}^1$) and $Co_{1-x}Fe_xS_2$; the orbital angular momentum operator has no nonzero matrix elements in the Γ_3 manifold.

Turning to the dipolar case, we note that $F(\Gamma_3) \sim 0.8$, assuming very small admixtures of Γ_5 and omitting electron-nucleus flip-flop transitions as appropriate for FM systems [32]. It follows that the dipolar mechanism plays an important role in nuclear relaxation in these materials. We take $\langle 1/r^3\rangle_F = \xi\langle 1/r^3\rangle_{\mathrm{atom}}$, with the parameter $\xi \sim 0.75$, as estimated for Co metal by Moriya [33]. This assumes that the wave functions at the Fermi surface are compact atomlike functions and this is supported by the neutron data [26,27].

The quantity κ plotted versus x in Fig. 2 (inset) may be expressed as

$$\kappa = 1/T_1T = C[\rho_\uparrow^2(x, E_F) + \rho_\downarrow^2(x, E_F)], \qquad (3)$$

with $C = 4\pi\mu_0^2\gamma_S^2\gamma_I^2\hbar^3 k_{\mathrm{B}}\langle 1/r^3\rangle_F^2$ $F(\Gamma) = 3.8 \times 10^{-37}\,\mathrm{J^2\,s^{-1}\,K^{-1}}$. We put $\rho_{\mathrm{NMR}}(E_F) = \sqrt{\kappa/C} = [\rho_\uparrow^2(x, E_F) + \rho_\downarrow^2(x, E_F)]^{1/2}$, and values obtained using the measured κ and calculated C are plotted in Fig. 3. Band structure calculations [14,15] and PCAR measurements [15] show that, for $x > 0.07$, $\rho_\uparrow(E_F) \gg \rho_\downarrow(E_F)$, implying $\rho_{\mathrm{NMR}}(E_F) \rightarrow \rho_\uparrow(E_F)$. For $x < 0.07$, both spin sub-bands are expected to make significant contributions to relaxation.

Also shown in Fig. 3 are values $\rho_{\mathrm{SH}} = [\rho_\uparrow(E_F) + \rho_\downarrow(E_F)]$, obtained from the low-temperature specific heat measurements, using $\gamma_e = (1/3)\pi^2 k_{\mathrm{B}}^2[\rho_\uparrow(E_F) + \rho_\downarrow(E_F)]$, and band structure values ρ_{BS} from theoretical LSDA calculations [35]. The agreement in the experimental values is evident and the curves follow the trend predicted by theory, with the DOS decreasing with x and reaching a plateau value near $x = 0.15$. These results demonstrate the utility of NMR for determining the composition dependence of the d-band DOS and add weight to our simple picture for the x-dependent evolution of the SP. For $x > 0.07$, the NMR DOS values obtained from $\sqrt{\kappa/C}$ are consistent with $\rho_\uparrow(E_F) \gg \rho_\downarrow(E_F)$ in the alloy system corresponding to a highly SP phase in agreement with the PCAR measurements. At lower $x < 0.07$ ρ_{NMR} and ρ_{SH} both increase. While the excellent quantitative agreement of the NMR and specific heat values for $\rho(E_F)$ may be somewhat fortuitous, in view of uncertainties in the NMR parameters in the constant C, the trends with x provide

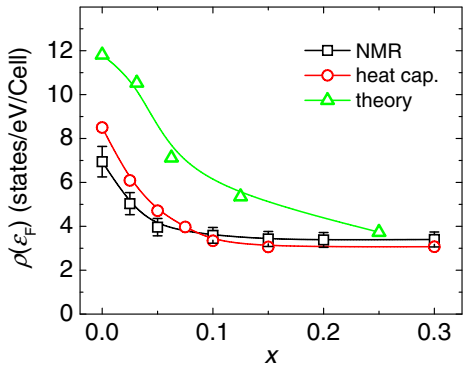

FIG. 3 (color online). DOS at the Fermi level $\rho(E_F)$ in $Co_{1-x}Fe_xCoS_2$ as a function of x. For $x > 0.07$, $\rho(E_F) \rightarrow \rho_{\uparrow}(E_F)$, the DOS for the majority spin sub-band. The values ρ_{NMR} obtained in the present work are calculated from the product κ of Fig. 2 using Eq. (2). The corresponding DOS results obtained from heat capacity measurements ρ_{SH} and band structure calculations ρ_{BS} (Ref. [33]) are shown for comparison.

important information on the evolution of the d-band electronic structure with Fe concentration. In particular, if the assumption concerning the e_g functions is not fully justified and the orbital mechanism plays a role in relaxation, slightly larger values for $F(\Gamma)$ could apply but the main conclusions of our analysis will not change.

In conclusion, the ^{59}Co NMR line shape and relaxation rate measurements made in low magnetic fields on FM samples of CoS_2 and $Co_{1-x}Fe_xS_2$ have provided useful information on the hyperfine interactions and the spin-lattice relaxation mechanism in these interesting itinerant FM materials. Analysis of the relaxation data has allowed us to extract the d-band DOS at the Fermi level as a function of x for these systems. The results correlate well with theoretical band structure calculations and support experimental magnetization and transport measurements that suggest high SP in the alloyed materials for $x > 0.07$ [15]. Although NMR does not distinguish between carriers with different spin, the technique in combination with other experiments that determine the spin polarization provides useful information for highly SP systems.

This work is supported by the NSF under agreement DMR-0084173. Work at UMN supported by the NSF MRSEC under Grant No. DMR-0212302. Helpful discussions with Dr. P. Schlottmann are gratefully acknowledged.

[1] C. M. Fang, G. A. de Wijs, and R. A. de Groot, J. Appl. Phys. **91**, 8340 (2002).
[2] J. M. D. Coey and M. Venkatesan, J. Appl. Phys. **91**, 8345 (2002).
[3] R. A. de Groot, F. M. Mueller, P. G. van Engen, and K. H. J. Buschow, Phys. Rev. Lett. **50**, 2024 (1983).
[4] S. A. Wolf, D. D. Awschalom, R. A. Buhrman, J. M. Daughton, S. von Molnár, M. L. Roukes, A. Y. Chtchelkanova, and D. M. Treger, Science **294**, 1488 (2001).
[5] I. Žutić, J. Fabian, and S. Das Sarma, Rev. Mod. Phys. **76**, 323 (2004).
[6] W. E. Pickett and J. S. Moodera, Phys. Today **54**, No. 5, 39 (2001).
[7] Yu. S. Dedkov, U. Rüdiger, and G. Güntherodt, Phys. Rev. B **65**, 064417 (2002).
[8] E. J. Singley, C. P. Weber, D. N. Basov, A. Barry, and J. M. D. Coey, Phys. Rev. B **60**, 4126 (1999).
[9] Y. Ji, G. J. Strijkers, F. Y. Yang, C. L. Chien, J. M. Byers, A. Anguelouch, G. Xiao, and A. Gupta, Phys. Rev. Lett. **86**, 5585 (2001).
[10] J. S. Parker, S. M. Watts, P. G. Ivanov, and P. Xiong, Phys. Rev. Lett. **88**, 196601 (2002).
[11] J.-H. Park, E. Vescovo, H.-J. Kim, C. Kwon, R. Ramesh, and T. Venkatesan, Nature (London) **392**, 794 (1998).
[12] B. Nadgorny, I. I. Mazin, M. Osofsky, R. J. Soulen, Jr., P. Broussard, R. M. Stroud, D. J. Singh, V. G. Harris, A. Arsenov, and Ya. Mukovskii, Phys. Rev. B **63**, 184433 (2001).
[13] I. I. Mazin, Appl. Phys. Lett. **77**, 3000 (2000).
[14] K. Ramesha, R. Seshadri, C. Ederer, T. He, and M. A. Subramanian, Phys. Rev. B **70**, 214409 (2004).
[15] L. Wang, K. Umemoto, R. M. Wentzcovitch, T. Y. Chen, C. L. Chien, J. G. Checkelsky, J. C. Eckert, E. D. Dahlberg, and C. Leighton, Phys. Rev. Lett. **94**, 056602 (2005).
[16] S. K. Kwon, S. J. Youn, and B. I. Min, Phys. Rev. B **62**, 357 (2000).
[17] T. Shishidou, A. J. Freeman, and R. Asahi, Phys. Rev. B **64**, 180401(R) (2001).
[18] L. Wang, T. Y. Chen, and C. Leighton, Phys. Rev. B **69**, 094412 (2004).
[19] P. Schlottmann, Phys. Rev. B **67**, 174419 (2003).
[20] P. A. Dowben and R. Skomski, J. Appl. Phys. **95**, 7453 (2004).
[21] C. P. Slichter, *Principles of Magnetic Resonance* (Springer-Verlag, New York, Berlin, 1990), 3rd ed.
[22] H. Hiraka and Y. Endoh, J. Phys. Soc. Jpn. **63**, 4573 (1994).
[23] E. Nowack, D. Schwarzenbach, and T. Hahn, Acta Crystallogr. Sect. B **47**, 650 (1991).
[24] A. Ohsawa, Y. Yamaguchi, H. Watanabe, and H. Itoh, J. Phys. Soc. Jpn. **40**, 986 (1976).
[25] A. Ohsawa, Y. Yamaguchi, H. Watanabe, and H. Itoh, J. Phys. Soc. Jpn. **40**, 992 (1976).
[26] H. Hiraka, Y. Endoh, and K. Yamada, J. Phys. Soc. Jpn. **66**, 818 (1997).
[27] H. Yasuoka, J. Phys. Soc. Jpn. **47**, 517 (1979).
[28] K. Adachi, K. Sato, M. Okimori, G. Yamauchi, H. Yasuoka, and Y. Nakamura, J. Phys. Soc. Jpn. **38**, 81 (1975).
[29] Although $1/T_1$ is proportional to T very small departures from a strict T dependence are found below 10 K. Experiments at $T < 1$ K are needed to investigate these effects.
[30] D. Hone, V. Jaccarino, T. Ngwe, and P. Pincus, Phys. Rev. **186**, 291 (1969).
[31] M. Shaham, J. Barak, U. El-Hanany, and W. W. Warren, Phys. Rev. B **22**, 5400 (1980).
[32] Y. Obata, J. Phys. Soc. Jpn. **18**, 1020 (1963).
[33] T. Moriya, J. Phys. Soc. Jpn. **19**, 681 (1964).
[34] D. O. Van Ostenburg, J. J. Spokas, and D. J. Lam, Phys. Rev. **139**, A713 (1965).
[35] K. Umemoto, R. M. Wentzcovitch, L. Wang, and C. Leighton (unpublished).